Available online at www.sciencedirect.com

ScienceDirect

Procedia Manufacturing 11 (2017) 641 – 649

Procedia MANUFACTURING

27th International Conference on Flexible Automation and Intelligent Manufacturing, FAIM2017, 27-30 June 2017, Modena, Italy

A design strategy based on topology optimization techniques for an additive manufactured high performance engine piston

Saverio Giulio Barbieri[a], Matteo Giacopini[a]*, Valerio Mangeruga[a], Sara Mantovani[a]

[a]*Dipartimento di Ingegneria "Enzo Ferrari", Università degli Studi di Modena e Reggio Emilia, via Vivarelli 10, 41125 Modena, Italy*

Abstract

In this paper, a methodology for the design of a motorcycle piston is presented, based on topology optimization techniques. In particular, a design strategy is preliminary investigated aiming at replacing the standard aluminum piston, usually manufactured by forging or casting, with an alternative one made of steel and manufactured via an Additive Manufacturing process. In this methodology, the minimum mass of the component is considered as the objective function and a target stiffness of important parts of the piston is employed as a design constraint. The results demonstrate the general applicability of the methodology presented for obtaining the geometrical layout and thickness distribution of the structure.

Peer-review under responsibility of the scientific committee of the 27th International Conference on Flexible Automation and Intelligent Manufacturing

Keywords: optimization; piston; topology; steel; engine; automotive.

1. Introduction

The piston represents the main alternating mass in an internal combustion engine mechanism. To minimize piston mass is therefore fundamental to contain inertial forces. Because of its low density, aluminium is the most common material employed for piston manufacturing. Unfortunately, aluminium exhibits low mechanical properties, which further decrease when it is exposed to high temperatures [1]. Turbocharging (downsizing), high compression ratios,

* Corresponding author. Tel.: +39-059-205-6112; fax: +39-059-205-6126.
E-mail address: matteo.giacopini@unimore.it

Peer-review under responsibility of the scientific committee of the 27th International Conference on Flexible Automation and Intelligent Manufacturing
doi:10.1016/j.promfg.2017.07.162

advanced spark ignition strategies are some of the techniques employed in modern engines in order to increase engine efficiency to fulfil strict norms on engine pollution emissions and to minimize fuel consumption. Therefore, higher specific loads could be encountered, which lead to higher mechanical and thermal loadings of engine components [2, 3]. In this scenario, aluminium may not represent the best choice and steel may be considered as a valid alternative for piston manufacturing. Schreer et al. [4] analysed the consequences of employing a steel piston: a better kinematic behaviour of the crank mechanism, a comparable weight, more homogeneous surface temperatures, a lower dead volume at the top land, a lower blow-by and a more efficient combustion process are the main advantages registered. Nevertheless, traditional manufacturing technologies cannot be employed when steel is considered as the material for pistons. In fact, in order to obtain components with a comparable weight when compared with those produced by aluminium, the thickness of the different parts of a steel piston have to be reduced up to one millimetre. Additive Manufacturing represents a promising technology to obtain thin features. Bendsøe and Kikuchi [5] related optimization techniques to structural design, noting that the resulting complex shapes could be easily reproduced by Additive Manufacturing. Du and Tao [6] and Zhao et al. [7] adopted the topology optimization for an engine piston lightening, but they used the results only to understand which parts of the piston were redundant, without ascribe any focused design validity. Brackett et al. [8] analysed the main challenges and opportunities for topology optimization for Additive Manufacturing. The importance of mesh resolution, manufacturing constraints and the post-processing have been highlighted.

In this contribution, topology optimization analyses are coupled with Finite Element analyses in order to reach an optimum steel piston configuration. In particular, the minimum mass of the component is considered as the objective function and the displacements of specific nodes on the piston skirt, crown and bosses are employed as design constraints. Different load cases are considered and the results of the topology optimization are revised and discussed with the prospective to employ Additive Manufacturing as the production technique.

2. Design strategy

2.1 Topology optimization

A generic optimization problem can be written in the form [9]

$$\begin{aligned} &\text{minimize}_{\boldsymbol{x}\in D}\, f(\boldsymbol{x}) \\ &\text{subject to } c(\boldsymbol{x})\geq 0 \end{aligned} \tag{1}$$

where the vector $\boldsymbol{x}$ represents a suitable parameterization of the problem, $\boldsymbol{D}$ is the design space, $f(\boldsymbol{x})$ is the objective function, and $c(\boldsymbol{x})$ are the constraints of the optimization. The functions $f(\boldsymbol{x})$ and $c(\boldsymbol{x})$ are usually computed via a suitable numerical technique while the optimization algorithm iteratively looks for the best configuration.

In topology optimization, since gradient information is readily available from the Finite Elements analyses, a large number of variables can be easily handled, accepting that a gradient-based optimization algorithm is adopted.

The most popular methods for topology optimization are the homogenization methods. In particular, in this paper the solid isotropic material with penalization methods, SIMP, is employed.

The theory of this method is described extensively by Bendsøe and Kikuchi [5] and Bendsøe and Sigmund [10]. The main scope of the method is to find the optimum material distribution in a structure. Finite Element analyses are performed assuming as a parameters vector the element-by-element relative material density, which is allowed to vary with continuity:

$$x = \{x_i \in (0,1], \forall i = 1, \dots, N)\} \tag{2}$$

where N is the number of finite elements in the structure.

The density of the i-th element is given by:

$$\rho_i\,(x_i) \;=\; x_i \rho^* \tag{3}$$

where ρ^* is the full density of the material. The material density and the material stiffness are correlated.

According to the homogenization method, the intermediate density material is treated as a homogeneous porous material with microscale voids, usually assumed to be rectangular. The local stiffness tensor of such a material is computed rigorously as a function of the holes shape, size, and orientation. This can involve a rather complicated mathematical procedure.

The SIMP method, which is adopted in this paper, is simpler, and assumes that the stiffness of the i-th element is given by

$$E_i(x_i) = x_i^p E^* \tag{4}$$

where E^* is the full stiffness of the isotropic material.

Two parameters control the behaviour of the algorithm: the penalty factor p, and the sensitivity filter r.

The penalty factor $p \geqslant 1$ appears in equation (4). Its role is to make intermediate densities unfavourable in the optimized solution. Setting the filter $r \geqslant 1$ the sensitivity of each element is averaged with the sensitivities of its surrounding elements within a radius equal r times the average mesh size, thus preventing the phenomenon of checkerboarding.

The objective of the optimizations is usually the minimization of the mass of the structure for a given displacement target. Larger values of p and r, despite reducing the performance of the structure in terms of objective function, make the solution physically meaningful. Thus, it is relevant to properly tune these parameters, also considering that inappropriate values of the parameters may affect the convergence of the optimization process negatively.

2.2 Model set up

The objective of the present work is the design of a steel piston for a four-stroke motorcycle engine.

For setting up a topology optimization problem, both the domain of the structure (design space) and the governing parameters, i.e. the objective and the constraints of the optimization, have to be defined.

The domain of the structure should be as wide as possible, according to the project restriction, in order to guarantee the maximum freedom to the optimization process in choosing the optimal material distribution.

Thus, the starting point in this study is a massive steel half cylinder representing a simple piston with a transversal hole and a parallelepiped pocket, useful to host the piston pin and the upper part of the connecting rod, see Fig. 1.

The adoption of a geometry as simple as possible is very important to achieve a regular high quality mesh. Sigmund and Petersson [11] and Zuo et al. [12] studied the mesh dependency of topology optimization results noting that different structural solutions can be obtained if different mesh size and quality are considered. Wankhade and Zolekar [13] used a more complex geometry of the piston, but in this case the ring belt belonged to the non-design space, so that this feature did not aggravate the analysis.

Fig. 1 shows the domain of the topology optimization. Purple elements describe the crown, the ring belt, the skirt and the pin boss and they are fixed, so that their density cannot be modified (non-design space). This layer is one millimeter thick and consists of about 187 thousand pentahedral elements (first order, 6 nodes, 6 Gaussian integration points). Orange elements form the bulk of the piston and represent the design space. The design space consists of 1.87 million tetrahedral elements (first order, 4 nodes, one Gaussian integration points), the average element size being one millimetre.

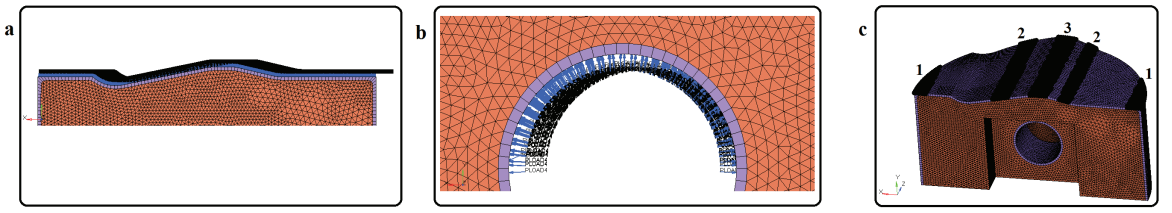

Fig. 1. domain of the topology optimization

The material considered for the analysis is a generic steel: Young modulus equal to 210000 MPa, density equal to 7.8 kg/dm^3 and Poisson's ratio equal to 0.3. It could seem wrong to use the property of a bulk isotropic material, because Additive Manufacturing techniques always produce anisotropic components due to their lay-up style process. Nevertheless Tolosa et al. [14] obtained selective laser molten steel with properties very close to the ones of the classic bulk material, even if an anisotropic behavior was always reported. Kruth et al. [15] studied the scanning strategies of Selective Laser Melting techniques. A thin wireframe structure, similar to the one typically resulting from optimization calculations, requires a short scan vector. Hence, adjacent tracks are scanned rapidly one after the other, leaving little cool down time in between, thus resulting in high temperatures. Consequently, suitable wetting conditions are present leading to a high density of the material. Kahlen and Kar [16] determined the yield and ultimate strength of laser-fabricated parts. The interface of two consecutive layers is not found to be the weakest joint. However, the maximum strength is found to occur in a direction, which is inclined at an angle with the direction of material deposition. This angle is influenced by the temperature gradient during the solidification of the melt pool. Gardan et al. [17] presented a numerical optimization method for improving the internal structure of models produced by additive manufacturing. They developed a system to manage the additive manufacturing process and the material characterization for a better integration with the topological optimization technique.

In the present contribution, the objective of the optimization is the minimization of the mass of the piston.

Several optimization constraints have been imposed, based on the deformations registered with Finite Element analysis of the original aluminium piston. In particular, three different load cases have been taken into account:

- top dead centre during combustion (*TDCC*)
- top dead centre at the beginning of the induction stroke (*TDCI*)
- instant of maximum piston thrust force (*PT*)

2.2.1 Top dead centre during combustion (TDCC)

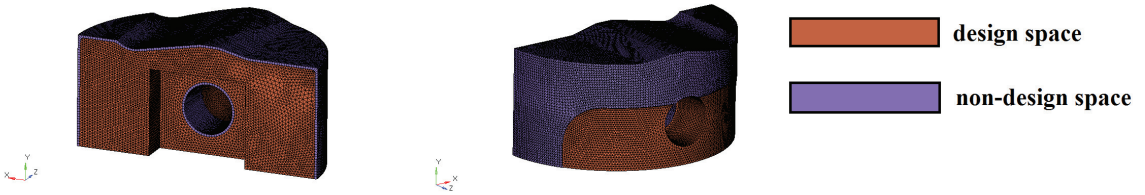

Fig. 2. (a) pressure on the piston top; (b) pressure on the pin boss; (c) nodes selected for design constrains

At *TDCC* the total force acting on the piston is about 40800 N. As a consequence, a pressure of about 5.23 MPa has been applied on the piston top while a pressure of about 71.8 MPa has been applied on the top half of the pin boss, see Fig. 2 (a) and (b). In this way, the piston results self-balanced. Proper symmetry constraints have been also applied.

Table 1 reports the design constraints limiting the deformation of the piston crown, see Fig. 2 (c), and considered to guide the process of optimization. The author acquired these values from a preliminary FEM analysis of the original aluminium piston in order to reach the same stiffness in the new component. The solver has been then forced to give a symmetric relative density distribution with reference to the piston *yz* plane.

Table 1. Values of design constraints at *TDCC*.

Nodes selected	Group 1	Group 2	Group 3
Lower bound (*mm*)	-0.02	-0.015	-0.01
Upper bound (*mm*)	0.001	0.001	0.001

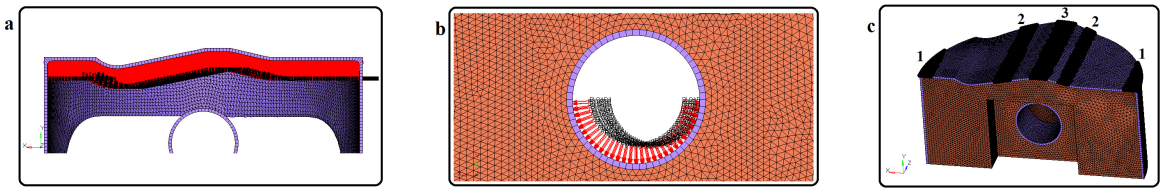

Fig. 3. (a) pressure on the piston top; (b) pressure on the pin boss; (c) nodes selected for design constrains.

2.2.2 Top dead center at the beginning of the induction phase (TDCI)

At *TDCI* the total force acting on the piston is about 18600 N. As a consequence, a pressure of about -2.4 MPa has been applied on the piston top while a pressure of about 27.17 MPa has been applied on the bottom half of the pin boss, see Fig. 3 (a) and (b). In this way, the piston results self-balanced. Proper symmetry constraints have been also applied.

Table 2 reports the design constraints limiting the deformation of the piston crown, see Fig. 3 (c), and considered to guide the process of optimization. The solver has been then forced to give a symmetric relative density distribution with reference to the piston *yz* plane.

Table 2. Values of design constraints at *TDCI*.

Nodes selected	Group 1	Group 2	Group 3
Lower bound (*mm*)	0.01	0.01	0.005
Upper bound (*mm*)	0.02	0.015	0.01

2.2.3 Instant of maximum piston thrust force (PT)

At *PT* the total force acting on the piston is about 4200 N. As a consequence, a pressure of about 42.2 MPa has been applied on the piston skirt while a pressure of about 7.9 MPa has been applied on a half side of the pin boss, see Fig. 4 (a) and (b). In this way, the piston results self-balanced. Proper symmetry constraints have been also applied.

Table 3 reports the design constraints limiting the deformation of the piston skirt, see Fig. 4 (c), and considered to guide the process of optimization. The solver has been then forced to give a symmetric relative density distribution with reference to the piston *yz* plane.

Table 3. Values of design constraints at *PT*.

Nodes selected	Group 1	Group 2	Group 3	Group 4	Group 5	Group 6	Group 7	Group 8	Group 9
Lower bound (*mm*)	-0.045	-0.04	-0.052	-0.057	-0.06	-0.075	-0.083	-0.09	-0.1
Upper bound (*mm*)	-0.035	-0.03	-0.042	-0.052	-0.05	-0.065	-0.073	-0.08	-0.09

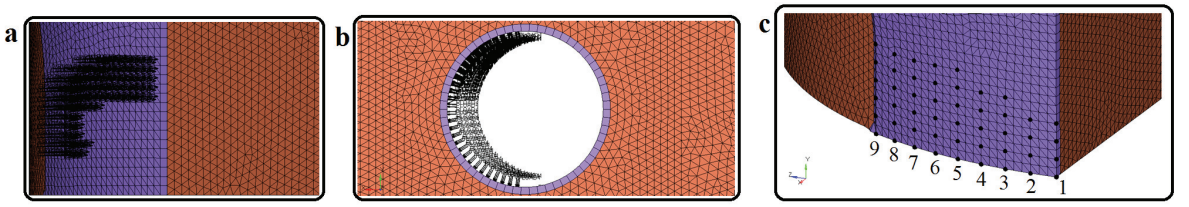

Fig. 4. (a) pressure on the piston skirt; (b) pressure on the pin boss; (c) nodes selected for design constrains.

2.3 The optimization process

The software package employed for the optimization is Altair OptiStruct 13, while the model set up has been made with Altair HyperMesh 13. In order to better calibrate the process, a sensitivity analysis on the optimization parameters DISCRETE (corresponding to the penalty factor, *p*) and MINDIM (related sensitivity filter, *r*) has been performed. The choice of the parameters has been driven by the following considerations:

- the solution achieved is more clearly defined;
- the number of intermediate density elements is lower;
- the convergence is achieved more easily;
- the topology of the piston is considered more interesting, innovative, and easier to be manufactured by the designer;

After the sensitivity analysis, it has been chosen to set the optimization parameters to DISCRETE=3 and MINDIM=2.

Despite the sensitivity analysis, the results of the topology optimization are still far from being ready-to-made solutions for the piston design: even if a suitable choice of the parameters is made, a certain number of elements having intermediate density always characterizes the results and there is no perfectly black-and-white solutions. Moreover, due to the domain discretization, the solution presents non-smooth surfaces. Therefore, the results have always to be interpreted in order to create new models, which have to be manually re-drawn using a CAD software. It could be possible to implement a proper filter to prevent the mesh-dependency and checkboard patterns, as reported by Hu et al. [18].

2.4 Results

The results of the optimization process has been discussed in terms of relative density contour plots. Each load case has been analysed independently in order to better understand how the density distribution is influenced by the load path and by the design constraints.

2.4.1 Top dead centre during combustion (TDCC)

The convergence of the iteration process has been achieved after 40 iterations.

Fig. 5 (a) shows elements with a relative density higher than 0.1. Ribs linking the pin boss to the crown are visible. Moreover, a wireframe structure is present in the area below the pin boss, where the solver leaves high-density elements as far as possible from the crown in order to increase the global bending stiffness of the piston.

Increasing the lower bound of the relative density up to 0.4, Fig. 5 (b), supports that are fundamental for the stiffness of the piston are clearly identified.

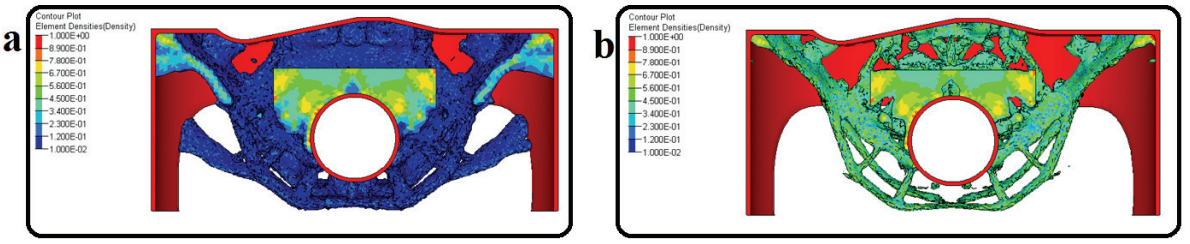

Fig. 5. (a) contour plot TDCC 0.1 density; (b) contour plot TDCC 0.4 density.

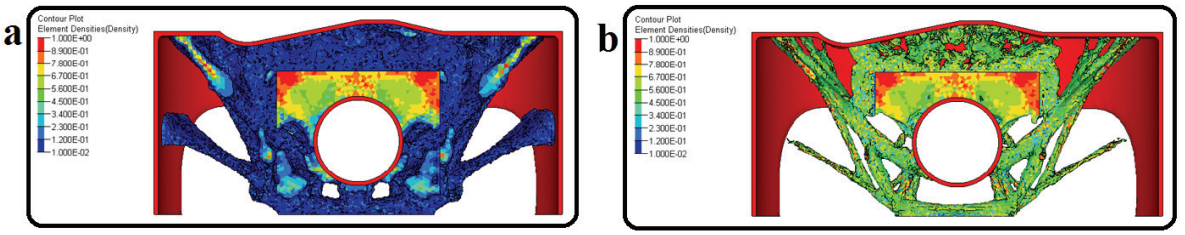

Fig. 6. (a) contour plot TDCI 0.1 density; (b) contour plot TDCI 0.5 density.

2.4.2 Top dead center at the beginning of the induction phase (TDCI)

The convergence of the iteration process has been achieved after 41 iterations.

Fig. 6 (a) shows elements with a relative density higher than 0.1. Ribs linking the pin boss to the crown are visible. Moreover, a wireframe structure is present in the area below the pin boss, where the solver leaves high-density elements as far as possible from the crown in order to increase the global bending stiffness of the piston.

Increasing the lower bound of the relative density up to 0.5, Fig. 6 (b), supports that are fundamental for the stiffness of the piston are clearly identified.

2.4.3 Instant of maximum piston thrust force (PT)

The convergence of the iteration process has been achieved after 16 iterations.

Fig. 7 (a) shows elements with a relative density higher than 0.1. Ribs linking the pin boss to the skirt are visible.

Increasing the lower bound of the relative density up to 0.4, Fig. 7 (b), supports that are fundamental for the stiffness of the piston are clearly identified.

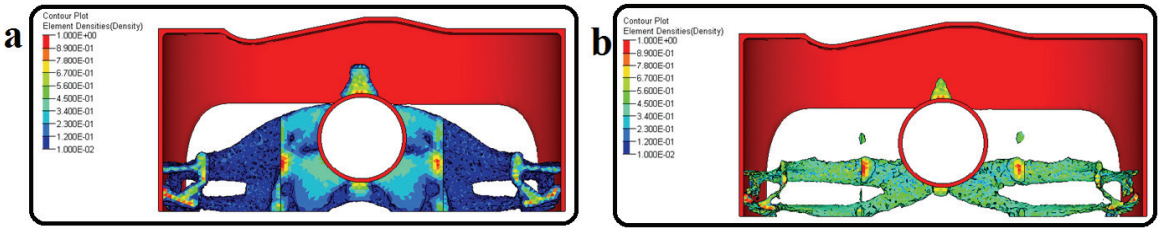

Fig. 7. (a) contour plot PT 0.1 density; (b) contour plot PT 0.4 density.

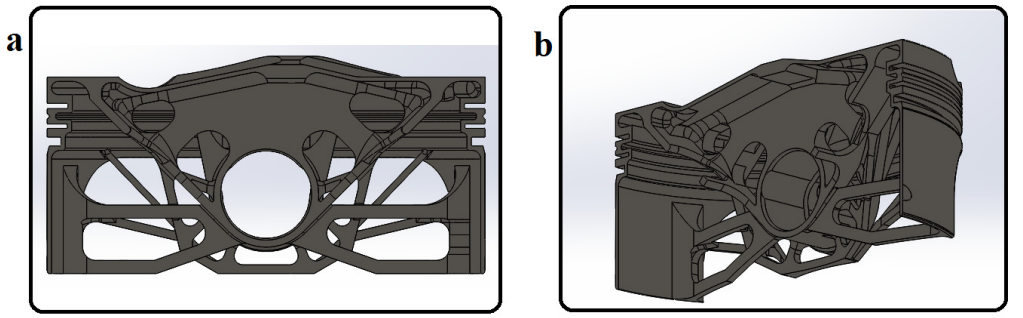

Fig. 8. (a) CAD model of the steel piston, view a; (b) CAD model of the steel piston, view b.

2.5 Post-processing

The next step of the methodology consisted in an interpretation of the results. Diaz and Sigmund [19] studied the checkerboard phenomenon that makes this interpretation process complicated. Zhou et al. [20] developed a new algorithm for a direct minimum member size calculation and checkerboard control that could lead to results easier to be interpreted by the designer. In the present paper, thanks to the preliminary sensitivity analysis on the parameters governing the optimization process, the different structural features are clearly visible for each load case result and they have been identified and employed to design a first proposal for the new steel piston, see Fig 8 (a) and (b).

3. Conclusion

A method for a computer aided steel piston design has been proposed. In particular, the presented methodology aimed at finding more efficient layout solutions for the piston framework feasible with Additive Manufacturing techniques. The authors employed topology optimizations to define the optimal structural topology. Special care has to be taken in setting up the optimization process since the choice of the constraints, i.e. the performance targets, of the mesh size and quality and of the optimization parameters directly affect the outcome of the process.

References

[1] M. Giacopini, S. Sissa, R. Rosi, S. Fantoni. Influence of different temperature distributions on the fatigue life of a motorcycle piston. Proceedings of the Institution of Mechanical Engineers, Part D: Journal of Automobile Engineering. 229 (9) (2015) 1276-1288.
[2] S. Sissa, M. Giacopini, R. Rosi. Low-cycle thermal fatigue and high-cycle vibration fatigue life estimation of a diesel engine exhaust manifold. Procedia Engineering. 74 (2014) 105-112.
[3] S. Fontanesi, M. Giacopini. Multiphase CFD-CHT optimization of the cooling jacket and FEM analysis of the engine head of a V6 diesel engine. Applied Thermal Engineering, 52 (2) (2013) 293-303.
[4] K. Schreer, I. Roth, S. Schneider, H. Ehnis. Analysis of aluminium and steel pistons – Comparison of friction, piston temperature and combustion. Journal of Engineering for Gas Turbines and Power. 136 (2014) 101506-1.
[5] M.P. Bendsøe, N. Kikuchi. Generating optimal topologies in structural design using a homogenization method. Computer methods in applied mechanics and engineering. 71 (1988) 197-224.
[6] F. Du, Z. Tao. Study on lightweight of the engine piston based on topology optimization. Advanced Materials Research. 201-203 (2011) 1308-1311.
[7] J. Zhao, F. Du, W. Yao. Structural analysis and topology optimization of a bent-bar-frame piston based on the variable density approach. ASME 2014 Dynamic Systems and Control Conference.
[8] D. Brackett, I. Ashcroft, R. Hague. Topology optimization for additive manufacturing. Proceedings of the Solid Freeform Fabrication Symposium. (2011) 348–362.
[9] M. Cavazzuti, A. Baldini, E. Bertocchi, D. Costi, E. Torricelli, P. Moruzzi. High performance automotive chassis design: a topology optimization based approach. Struct Multidisc Optim. 44 (2011) 45–56.
[10] M.P. Bendsøe, O. Sigmund. Topology optimization: theory, methods and applications, Springer, Berlin, 2004.
[11] O. Sigmund, J. Petersson. Numerical instabilities in topology optimization: a survey on procedures dealing with checkerboards, mesh-dependencies and local minima. Structural Optimization. 16 (1998) 68-75.
[12] K. Zuo, L. Chen, Y. Zhang, J. Yang. Study of key algorithms in topology optimization. Int J Adv Manuf Technol. 32 (2007) 787-796.

[13] L.N. Wankhade, V. Zolekar. Finite Element analysis and optimization of i.c. engine piston using RADIOSS and OptiStruct. Altair Technology Conference, 2013.
[14] I. Tolosa, F. Garciandìa, F. Zubiri, F. Zapirain, A. Esnaola. Study of mechanical properties of AISI 316 stainless steel processed by "selective laser melting", following different manufacturing strategies. Int J Adv Manuf Technol. 51 (2010) 639-647.
[15] J. P. Kruth, L. Froyen, J. Van Vaerenbergh, P. Mercelis, M. Bombouts, B. Lauwers. Selective laser melting of iron-based powder. Journal of Materials Processing Technology 149 (2004) 616–622.
[16] F. J. Kahlen, A. Kar. Similarity Parameters for Rapid Manufacturing. Journal of Manufacturing Science and Engineering. 123 (2001) 38-44.
[17] N. Gardan, A. Schneider, J. Gardan. Material and process characterization for coupling topological optimization to additive manufacturing. Computer-Aided Design and Applications, 2015.
[18] S.B. Hu, L.P. Chen, Y.Q Zhang, J. Yang, S.T. Wang. A crossing sensitivity filter for structural topology optimization with chamfering, rounding, and checkboard-free patterns. Struct Multidisc Optim. 37 (2009) 529-540.
[19] A. Dìaz, O. Sigmund. Checkerboard patterns in layout optimization. Structural Optimization. 10 (1995) 40-45.
[20] M. Zhou, Y.K. Shyy, H.L. Thomas. Checkerboard and minimum member size control in topology optimization. Struct Multidisc Optim. 21 (2001) 152–158.